

UNIVERSIDADE DE SÃO PAULO

INSTITUTO DE FÍSICA
CAIXA POSTAL 20516
01498 - SÃO PAULO - SP
BRASIL

PUBLICAÇÕES

IFUSP/P-926

FUSION OF ^{59}Co WITH LIGHT PROJECTILES AT
NEAR BARRIER ENERGIES

P.R.S. Gomes, T.J.P. Penna

Departamento de Física, Universidade Federal Fluminense
24020 Outeiro São João Batista, Niterói, R.J., Brazil

E.F. Chagas

Instituto Tecnológico de Aeronáutica, C.T.A.
12200 São José dos Campos, S.P., Brazil

**R. Liguori Neto, J.C. Acquadro, P.R. Pascholati, E. Crema,
C. Tenreiro, N. Carlin Filho, M.M. Coimbra**
Instituto de Física, Universidade de São Paulo

Julho/1991

FUSION OF ^{59}Co WITH LIGHT PROJECTILES AT NEAR BARRIER ENERGIES

P.R.S. Gomes⁺, T.J.P. Penna⁺

Departamento de Física, Universidade Federal Fluminense
24020 Outeiro São João Batista, Niterói, R.J., Brazil

E.F. Chagas

Instituto Tecnológico de Aeronáutica, C.T.A.
12200 São José dos Campos, S.P. Brazil

R. Liguori Neto, J.C. Acquadro, P.R. Pascholati⁺, E. Crema
C. Tenreiro, N. Carlin Filho, M.M. Coimbra^{*}

Instituto de Física, Universidade de São Paulo
C.P. 20516, 01498 São Paulo, S.P., Brazil

⁺Fellow of CNPq.

^{*}Present address: Instituto de Física, Universidade Estadual de Londrina, PR, Brazil.

ABSTRACT

Fusion cross sections have been measured for the ^{14}N , $^{16}\text{O}+^{59}\text{Co}$ systems at bombarding energies from 32 MeV to 56 MeV. Total transfer cross sections to excited states were simultaneously measured for the stripping of one proton and stripping of one neutron channels in the ^{14}N induced reactions, and their upper limits for other transfer channels could be estimated. The elastic scattering angular distribution was measured at $E_{\text{lab}} = 40$ MeV for the $^{16}\text{O}+^{59}\text{Co}$ system. The effects of collective properties of the nuclei, included in the Wong model or the alternative approach of coupling inelastic models, were found to be too small to explain the large sub-barrier fusion cross section enhancement. In order to perform simplified coupled channel calculations involving transfer channels, a semiclassical formalism was used to derive the transfer form factors. Within the uncertainties of the calculations, the behavior of the sub-barrier fusion could be understood in terms of the coupling of charged particle transfer channels, particularly the stripping of multi-nucleons, which act as doorways to fusion. An alternative approach, the liquid drop model, which accounts for the neck formation, also leads to satisfactory and compatible results.

PACS: 20.25.70.Jj, 20.25.70.Cd, 20.24.10.Eg

1. Introduction

The enhancement of the fusion cross sections at sub-barrier energies, relative to the predictions of unidimensional barrier penetration models is well established^{1,2}; at the present time most of the efforts in the field of heavy ion reactions around the Coulomb barrier is concerned with the study of the interplay between different reaction mechanisms and how they influence one another. Recent studies show that the fusion cross section depends intimately on the presence of other reaction channels^{3,4}, but the understanding of that, and particularly the influence of quasi-elastic transfer channels on fusion, is still very far off.

If fusion is a multi-step process, with a transfer channel with positive Q -value as a doorway to fusion, the available energy of the system, relative to the Coulomb barrier, will be increased and the fusion cross section may be enhanced. It can be shown⁵ that channels with negative Q -values may also enhance the fusion cross section. Therefore, the coupling of transfer channels, which can be considered a microscopic view of the neck formation, has the same net effect of splitting and lowering the Coulomb barrier as does the coupling of inelastic channels.

There are important experimental results, e.g. the study of the $^{58,64}\text{Ni} + ^{58,64}\text{Ni}$ systems^{6,7}, indicating that systems with large transfer cross sections have large sub-barrier fusion enhancements. One has to be careful when relating fusion and transfer cross sections, because they may take place at different distances and be sensitive to the form of potentials and form factors at regions where they are quite different. Depending on the relations between the average transfer distance and the distance where fusion starts to occur, the transfer mechanism may contribute to the fusion enhancement or, in an opposite way, absorb part of the flux which would go to the fusion channel. In a microscopic view, the neck formation process increases the distance of no return from fusion.

One has also to study the role played by ground state transfer Q -values (Q_{gg}) and

effective Q -values (Q_{eff}) on the fusion process. Q_{eff} is defined as

$$Q_{eff} = Q_{gg} + \Delta E_c \quad (1)$$

where ΔE_c is the variation of the Coulomb barrier between the entrance and the exit channels of a transfer process which acts as a doorway to fusion.

A suitable approach to investigate the influence of transfer channels on the fusion cross section is the coupled channel treatment, which has, however, many associated difficulties. In a complete calculation many inelastic couplings should be included, as well as all the important reaction channels, which are very difficult to predict. The analysis is, therefore, quite long and the problem can not be fully solved since some truncation has to be assumed. There are also uncertainties coming from the folding potentials or empirically determined nucleus-nucleus potentials used, which may have asymptotic values quite different from those when the nuclei overlap. Another critical source of uncertainty in the treatment is the value of the transfer coupling strength to be used.

In the study of the fusion problem in a coupled channel approach, the use of approximations and simple assumptions, as in the CCFUS code^{5,8} is widespread. This code is very simple and attractive because it gives at least a good qualitative idea of the influence of different coupling channels on the fusion process, and it has given good results for a large variety of systems to which it has been applied.

Another approach to the study of the sub-barrier fusion enhancement is the search for degrees of freedom which may influence the fusion mechanism by splitting and lowering the Coulomb barrier, such as the deformation of the nuclei, their surface vibrations and the neck formation process. The uncertainties from the potentials to be used are also present, as well as the difficulties in isolating the effects of the different degrees of freedom.

Most of the systems studied so far are concerned with medium and heavy nuclei, where the sub-barrier fusion enhancements are remarkable. In order to investigate

the influence of transfer channels on the fusion of light-heavy ion systems, we have performed experiments with ^{14}N and ^{16}O projectiles on a ^{59}Co target, which has a missing $f_{7/2}$ proton to complete the shell with $Z = 28$. For the ^{14}N induced reactions there are channels with positive Q_{gg} -values, whereas all transfers of one and two particles for the ^{16}O projectile have negative Q_{gg} -values, although there are channels with positive Q_{eff} -values. In table 1 the Q_{gg} and Q_{eff} -values of transfer channels of one and two nucleons and one alpha particle are listed, for both systems.

For the $^{16}\text{O}+^{59}\text{Co}$ system, for which both fusion and elastic scattering data were available, we have also used a third approach to describe the sub-barrier fusion behavior⁹, based on an optical model analysis¹⁰. The results showed that the fusion process is decided at large distances, close to the Coulomb barrier, compatible with the interpretation that neck formation leading to fusion can occur at those distances.

In section 2 of this paper we present the experimental data. In section 3 the fusion excitation functions are analysed by barrier penetration models and additional degrees of freedom such as dynamical deformations and neck formation. In section 4, coupled channels calculations are presented, including inelastic and transfer channels. Approximate transfer form factors are derived through a semiclassical formalism. In section 5 conclusions are drawn.

2. Experiments and Results

The experiments were performed at the S. Paulo Pelletron accelerator, and the energy range of the ^{14}N and ^{16}O beams was from 32 to 56 MeV, for the fusion and transfer reactions. The angular distribution of the elastic scattering with ^{16}O was measured at the laboratory energy of 40 MeV. The beam energy resolution was of the order of 10^{-3} .

2.1. FUSION AND TRANSFER

The fusion and transfer cross sections were determined by the in-beam and off-beam gamma-ray spectroscopy methods, described in details elsewhere¹¹, which allow the simultaneous measurement of fusion, transfer channels and inelastic scattering cross sections. The transfer cross sections determined are a lower limit of the total transfer yield, since they correspond to transfer processes leading to the excited states from which gamma transitions are detected.

The targets consisted of pure metallic cobalt, with thicknesses in the range 200 - 400 $\mu\text{g}/\text{cm}^2$, evaporated on Pb backings thick enough to stop the beam, in order to avoid Doppler shifts of the γ lines. For each bombarding energy a different target was used, avoiding undesirable contributions to the spectra coming from the decay of previous irradiations. The mean beam energy loss in the target was typically of the order of 0.3 - 0.4 MeV.

Fusion cross sections were obtained by adding up to 13 evaporation channels in the ^{14}N induced reaction, and up to 9 channels in the ^{16}O case. Evaporation channels of two, three and four particles were identified. The channels with higher cross sections were pn , $p2n$, $2pn$ for nearly the entire energy range and α (or $2p2n$), αpn , $\alpha p2n$ and $\alpha 2p$ at the highest energies. These results are in agreement with the predictions of the evaporation code PACE¹². The evaporation cross sections determined by the off-beam method correspond to the pn , $2pn$, and αn channels for ^{16}O and $p2n$ and $\alpha p2n$ for the ^{14}N case. Table 2 shows the measured fusion cross sections for the ^{14}N and ^{16}O induced reactions.

The γ lines of the ^{59}Co nucleus, corresponding to inelastic excitations, were found to be of very small intensities and/or not resolved from transitions of the evaporation channels (1098 keV and 1190 keV) or strong background lines (1460 keV from ^{40}K). As a consequence, the inelastic scattering cross sections were not determined in this work.

Two transfer channels were identified and had their cross sections measured for the ^{14}N induced reactions: the stripping of one proton ($-1p$) and of one neutron ($-1n$). The $-1p$ channel was identified by 3 transitions of the ^{60}Ni nucleus, and its cross section was determined by the line of 1332 keV, corresponding to the $2_1^+ \rightarrow 0^+$ transition. The $-1n$ channel was identified by 5 transitions of the ^{60}Co nucleus. The first excited state of this nucleus has an excitation energy of 58 keV and could not be detected by our experimental set-up. For the pick up of one neutron ($+1n$) channel, in the $^{14}\text{N}+^{59}\text{Co}$ system, the first 3 excited states of ^{58}Co are below the energy region of the detected γ rays, and therefore we could not say anything about its cross-section. For all the other transfer channels in both ^{14}N and ^{16}O induced reactions, there were no identified γ lines. The upper limit for their cross sections could be estimated, from the analysis of the gamma-ray spectra, to be in the range from 2.0 to 5.0 mb, at energies close to the barriers. The measured transfer cross sections to excited states are presented in table 2.

2.2. ELASTIC SCATTERING

The angular distribution of the elastic scattering of $^{16}\text{O}+^{59}\text{Co}$ was measured at one energy, just above the Coulomb barrier ($E_{\text{lab}} = 40$ MeV), in the angular range from 50° to 170° in the laboratory, by using an array of four Si surface barrier detectors with energy resolution of 500 keV. The inelastic scattering peak was found to be negligible, as already observed with the γ method. Two other detectors were placed at $\pm 25^\circ$ and were used as monitors. The elastic scattering of this system has been previously studied by Tannous et al.¹³ at bombarding energies from 36 to 56 MeV, with angular steps larger than in this work. The angular distributions at $E_{\text{lab}} = 40$ MeV of both works agree very well.

3. Analysis of the Fusion Excitation Function by Barrier Penetration Models

3.1. UNIDIMENSIONAL PENETRATION MODELS

As a preliminary analysis of the fusion excitation functions, only the data corresponding to cross sections above 50 mb were considered, in order to derive the barrier parameters V_B , R_B and $\hbar\omega$, the height, radius and curvature of the barrier, respectively, by the use of unidimensional barrier penetration models (UBPM). Calculations were performed with the nuclear potentials of Krappé-Nix-Sierk (KNS)¹⁴ and the proximity potential of Blocki¹⁵. The values obtained are shown in table 3. The free parameter Δr is the variation of the radius of each nucleus, needed to reproduce the data at high energies. The mean values of the barrier parameters obtained from a systematic study of Vaz et al.¹⁶, for V_B and R_B , and Reisdorf et al.¹⁷ for $\hbar\omega$ are given in table 3. From the table one can see that the barrier parameters are not very sensitive to the particular form of potential used.

The experimental fusion cross section at sub-barrier energies is underestimated when one uses either of the UBPM mentioned. Figure 1 shows the fusion data and the predictions of the KNS model for both systems.

For the $^{16}\text{O}+^{59}\text{Co}$ system, where there are fusion data at sufficiently low energy, one can determine the asymptotic energy shift ΔD_{exp} defined as¹⁸ the energy shift, at very low energies, needed in the UBPM calculation to force agreement with the experimental data. A value of $\Delta D_{\text{exp}} = 1.25 \pm 0.10$ MeV was found. This quantity can be used as a measure of the fusion cross section enhancement; a systematic study¹⁹ shows that it increases with the size of the system. The analysis of the quantity $\eta = \Delta D_{\text{exp}}/V_b$ can be, however, a more suitable way of measuring the relative importance of the fusion cross section enhancement. For the $^{16}\text{O}+^{59}\text{Co}$ system, $\eta = 4.1\%$, which is a large value, even when compared with much heavier systems.

3.2. ADDITIONAL DEGREES OF FREEDOM

The first approach used to try to explain the sub-barrier fusion cross section enhancement was the Wong model with deformation²⁰, where the dynamics of the system is considered through an effective deformation of the colliding nuclei, which accounts for the surface vibration of the nuclei (dynamical deformation) and changing orientation (static deformation). For spherical projectiles there are four parameters in this model, the three barrier shape parameters, obtained from the data above the Coulomb barrier, and one free parameter, the effective quadrupole deformation of the target nucleus, $\beta_{2\text{Wong}}$. The fit of the full excitation function is performed by allowing small variations in the pre-determined barrier parameters, and with the free $\beta_{2\text{Wong}}$. The value of $\beta_{2\text{Wong}}$ obtained from the best fit must then be compared with the predictions from other methods such as Coulomb excitation and scattering of light particles. For both systems studied, the derived values of $\beta_{2\text{Wong}}$ were identical, within the error bars: 0.266 ± 0.025 and 0.263 ± 0.017 for ^{16}O and ^{14}N induced reactions, respectively.

The deformation of the ^{59}Co nucleus was derived from the expression²¹

$$\beta_2 = (5\pi/9)^{1/2} (Q_0/Z) R_0^2 \quad (2)$$

where Q_0 is the intrinsic quadrupole moment and $R_0 = 1.2 A^{1/3}$. From the value of $(Q_0/Z)R_0^2 = 8.8 \times 10^{-2}$,²² one obtains $\beta_2(^{59}\text{Co}) = 0.116$, which is much smaller than the value $\beta_{2\text{Wong}}$ needed to fit the data. One can conclude that the Wong model does not give a reasonable description of the fusion data for the systems, as can be seen from figure 2, where the large dashed lines are the predictions of this model when one uses the deformation value $\beta_2(^{59}\text{Co})$. The associated asymptotic energy shift for the $^{16}\text{O}+^{59}\text{Co}$ system is $\Delta D_{\text{Wong}} = 0.25$ MeV, much smaller than the experimental one.

Another degree of freedom must, therefore, contribute to the enhancement of the sub-barrier fusion cross section. We have applied the liquid drop model approach,

developed by Aguiar et al.¹⁸, where the neck formation is considered, with the net effect of decreasing the fusion barrier by an amount ΔB . In this model a neck coordinate is introduced and it is shown that the system finds no barrier for a motion along the neck when it has enough energy to reach a certain critical separation which is larger than the fusion barrier. The authors suggest that this effect describes the background behavior associated with the bulk properties of nuclear matter, and that it depends on the size of the system. Strong collective couplings would be responsible for some extra enhancement of the fusion cross section. From a systematic study of heavy systems¹⁹ they associate the quantity ΔB with the general trend of the experimental asymptotic energy shift ΔD_{exp} and parametrize ΔB by the expression

$$\Delta B = 0.0016 \zeta^{2.5} \text{MeV} \quad (3)$$

where ζ is a measure of the size of the system.

As the effects of the nuclear structure of the collision nuclei for $^{16}\text{O}+^{59}\text{Co}$ did not appear to be important, one should expect, from the liquid drop model, that ΔD_{exp} would be a value close to that predicted by expression (3). Actually, for this system, $\zeta = 13.8$ and the value of ΔB , which will be called ΔD_{neck} in this paper, is 1.13 MeV, which is very close to $\Delta D_{\text{exp}} = 1.25 \pm 0.10$ MeV. The dynamical deformation of the nuclei contributes with a small energy shift $\Delta D_{\text{Wong}} = 0.25$ MeV.

Therefore, one can conclude that for this light system the neck formation is the main reason for the sub-barrier fusion enhancement.

In the next step of the analysis we perform coupled channel calculations, with the aim of understanding the fusion process by a more microscopic approach, and trying to show the equivalences of the Wong model and neck formation process with the coupling of inelastic and transfer channels, respectively.

4. Coupled Channel Calculations

4.1. COUPLING OF INELASTIC CHANNELS

The coupling of inelastic channels on the fusion process is an alternative approach to the Wong model, since the dynamics of the interactions, such as rotational and vibrational bands, is considered when one couples inelastic channels. Within this treatment one decomposes the multicomponent wave function into channel eigenstates, introducing a channel eigenstate dependent barrier. The C.C. treatment has limitations, as already mentioned in section 1 of this paper, and we are going to use a simplified code CCFUSB^{5,8,23} in the following analysis, which makes it just a good approximation of the full C.C. problem. The code CCFUSB²³ is an improvement of the finite range version⁵ of the original constant coupling approximation of the CCFUS code⁸. The main modifications introduced in CCFUSB are described in reference 24.

The inelastic channels considered were the first excited state of the projectile (0^+ at $E_x = 2.31$ MeV, and 3^- at $E_x = 6.13$ MeV, for ^{14}N and ^{16}O , respectively), and the first four excited states of the ^{59}Co target. The B(E2) and B(E3) values to the ground state transitions were used to derive the deformation lengths through the usual relations^{8,21}, the coupling strengths were also obtained from the usual expression⁸. The single coupling which gives the largest fusion enhancement is the $9/2$ state of the ^{59}Co nucleus, at $E_x = 1190$ keV, which has a relatively strong E2 transition ($\beta_2 = 0.1054$, from ref. 26).

Figure 2 also shows the results of the coupled channel calculations for both systems. The asymptotic shifts ΔD_{in} were found to be 0.078 and 0.058 MeV for the ^{16}O and ^{14}N induced reactions, respectively. When one couples only the inelastic channels corresponding to the excitations of target with the strongest B(E2) values, the calculations lead essentially to the same results, showing that there is no need to couple too many weak channels. One can see that, as in the Wong model,

the coupling of inelastic channels underestimates the experimental fusion cross sections, and that transfer channels should also be coupled in order to try to fit the data. As expected, both approaches lead to similar results, within the limitations and approximations used.

The failure of the coupling of inelastic channels and the Wong model to predict the experimental fusion cross sections are consistent with the observation of very small inelastic cross sections, which are both caused by the small collectivity of the ^{59}Co nucleus, giving rise to weak transition probabilities B(E2). The neck formation, or alternatively, the coupling of transfer channels, should be, in this situation, the main reason for the fusion cross section enhancement.

4.2. DETERMINATION OF TRANSFER FORM FACTORS

The main uncertainties in the coupled channel treatment, which includes transfer channels, are the transfer form factors which should be used. In the following we use a simplified semiclassical formalism, suggested by Corradi et al.²⁴ and improved by Winkelman et al.²⁵, to extract, approximately, the form factor for different transfer channels which had their cross sections measured or upper limits estimated. Additional information coming from experimental angular distributions of elastic scattering, which are available for one of the systems studied, are also used.

With semiclassical conditions fulfilled (Sommerfeld parameters around 20), one can consider localized classical trajectories, and, as the orbits remain outside the range of nuclear forces, Rutherford orbits can be assumed, although corrections due to the tail of the nuclear potential are also introduced. As a consequence, only the exponential tails of the form factors are relevant to the following analysis. At low energies, not too much above the Coulomb barrier, the following ansatz for the form factor is made:

$$F(r) = F_0(\varphi(r)/r) \exp(-\alpha(r - D_c)) , \quad (4)$$

where $D_c = d_c(A_1^{1/3} + A_2^{1/3})$ is a core parameter, α is the slope parameter, F_0 is the form factor constant and $\varphi(r)$ is a smooth function which limits $F(r)$ towards

a maximum close to the Coulomb barrier. The value of F_0 is defined when one normalizes the transfer cross sections predicted by this formalism to the measured ones. In the following we describe briefly the procedure used to extract the form factors. More general and detailed descriptions are found in references 24 and 25. The calculations were performed by the SBTRANS code²⁷.

In a general situation one defines the absorption probability as

$$P_a(\theta) = 1 - d\sigma_{el}/d\sigma_{Ruth} \quad (5)$$

This probability depends on the distance of closest approach $D(\theta)$ and it can be parametrized, neglecting rainbow effects, as

$$\begin{aligned} (D \geq D_a) \quad P_a(D) &= 0 \\ (D_c \leq D \leq D_a) \quad P_a(D) &= 1 - ((D - D_c)/(D_a - D_c))^{*s} \end{aligned} \quad (6)$$

where $D_a = d_a(A_1^{1/3} + A_2^{1/3})$ is the absorption distance parameter and s is the absorption slope at D_a . The parameters d_a and s can be derived from the experimental elastic scattering angular distributions.

Figure 3 shows the $d\sigma_{el}/d\sigma_{Ruth}$ data taken from this work and from reference 13, at $E_{lab} = 40$ MeV, plotted as a function of the reduced distance of closest approach d . The value of $d_a = 1.74$ fm is extracted directly from the figure. Two different fits were made: (i) following the prescriptions of references 24 and 25, the value of $d_c = 1.40$ fm was kept fixed, because this is the value found for several other systems, the fit leads to $s = 0.66/\text{fm}$. (ii) d_c was set as free parameter, when the values of $d_c = 1.425$ fm and $s = 0.61/\text{fm}$ were found. Both fits are similar, within the experimental errors. Running the SBTRANS for both sets of values, the final results for the form factors were found to be almost unaffected, as could be expected, since most of the transfer events occurs at distances much larger than D_c . The first set was used in the following analysis.

The slope parameters of the form factors are calculated from the binding energies E_B , through the expression $\alpha_{gg} = (2mE_B)^{1/2}/\hbar$. These values are corrected, to take into account the dependence on the excitation energies, by averaging the values of α at the initial and final reaction channels. Excitation energies up to 10 MeV were considered and a simple weight function $\rho(E_x) = 1/\text{MeV}$ was used. The corrections lead to average α which are typically of the order of 5% smaller than the ground state value α_{gg} . For charged particle transfer channels, corrections are made to the binding energies, in order to take into account the Coulomb barrier and the Coulomb field of the approaching nuclei.

This treatment is valid only for single step transfer processes. However it has already been shown²⁸ that when projectile and target are not deformed, a sequential transfer of two single nucleons obey the relation $\alpha_{2nucl} = 2\alpha_{1nucl}$. As neither of the nuclei involved in this work is deformed, we have used this relation to determine the slopes for transfer of two protons and two neutrons. For the transfer of pn we have considered two different situations: a sequential transfer, where the slope is defined as $\alpha_{pn} = \alpha_p + \alpha_n$, and the transfer of one deuteron, where the binding energy has been corrected as $BE(d) = BE(pn) - 2.2$ MeV. The differences were not pronounced, and in the following analysis, the direct transfer is assumed. For the transfer of one alpha particle, a direct transfer was considered, with the correction of the binding energy as $BE(\alpha) = BE(2p2n) - 28$ MeV.

The value of F_0 is obtained from the values of the experimental cross sections, for the channels which have been measured, or their upper limits estimated from the background analysis of the γ spectra, for the other channels. The calculations were performed at $E_{lab} = 34$ MeV and 40 MeV, for the ^{14}N and ^{16}O induced reactions, respectively, energies close to the Coulomb barriers. The estimated upper limits for the transfer cross sections to excited states were in the range from 2 to 5 mb for the different channels considered.

In order to take into account the contributions of the transfer cross sections which feed directly the nuclei ground states, a correction factor f was introduced. As an example, for the $^{58}\text{Ni} + ^{58,64}\text{Ni}$ systems, transfer cross sections were measured by both gamma²⁹ and particle⁷ detection, and f was found to be as large as 2.0.

4.3. COUPLING OF TRANSFER CHANNELS

a) $^{16}\text{O} + ^{59}\text{Co}$ system

From table 1 one can see that all the transfer channels considered have large negative Q_{gg} -values, but that there are two channels, $-\alpha$ and $-p$, which have positive Q_{eff} -values (4.86 and 0.28 MeV, respectively). From the experimental γ spectra no transfer channel could be identified, and only estimates of upper limits could be made. With the initial value of 2.5 mb for the cross sections of all the transfer channels considered, only for four stripping channels ($-\alpha$, $-1p$, $-2p$, $-d$) the SBTRANS code found values of F_0 which we could accept as realistic ($F(r_b) > 10$ were rejected, where $F(r_b)$ is the form factor at the barrier). Running the CCFUSB code, the very weak influence of the two channels with negative Q_{eff} -values ($-2p$ and $-d$) on the fusion cross section came out, and therefore only the $-\alpha$ and $-p$ channels were considered in the following analysis. Calculations were performed for transfer cross sections in the range from 2.5 to 5.0 mb, corresponding to a correction factor of $1.0 \leq f \leq 2.0$. It is interesting to note that the transfer of single nucleons ($+p$, $+n$) do not influence significantly the fusion cross section for this system.

In order to have an idea about the role of the coupling of each channel on the fusion process, calculations have been performed with the coupling of inelastic channels and each of these transfer channels. For the $-\alpha$, the average transfer distance was derived as $\langle d_t \rangle = 1.59$ fm, the slope of the form factor as $\langle \alpha \rangle = 1.55/\text{fm}$ and the asymptotic shift of the fusion cross section as $\Delta D_t(-\alpha) = 2.114$ MeV for $f = 2.0$, corresponding to a form factor at the barrier of $F(r_b) = 0.54$ MeV. This value of ΔD_t is quite large when compared with the one obtained only with inelastic

couplings ($\Delta D_{in} = 0.078$ MeV). For the $-p$ channel the values obtained were $\langle d_t \rangle = 1.67$ fm, $\langle \alpha \rangle = 0.675/\text{fm}$, $F(r_b) = 0.17$ MeV and $\Delta D_t(-p) = 0.105$ MeV. When both transfer channels are coupled, one obtains $\Delta D_t = 2.155$ MeV if $f = 2$ and 1.675 MeV if $f = 1$. The two dashed curves in figure 4 correspond to the results of such couplings for $f = 1.0$ and 2.0, respectively.

b) $^{14}\text{N} + ^{59}\text{Co}$ system

For this system we should not be able to follow the same procedure of analysis because there are neither elastic scattering nor low energy fusion data available. However, there should be no problem in using the same absorption parameters obtained from a similar system, due to the fact that small variations do not have a large effect on the determination of the form factors. Moreover, in this case, two transfer channels were identified experimentally, the $-1p$ and $-1n$, and there are four channels with positive Q_{gg} - and Q_{eff} -values (see table 1). Therefore, it is worthwhile to derive the transfer form factors and to study the predictions of the role played by those channels in the fusion cross section by coupled channel calculations.

Running the SBTRANS code, seven transfer channels were selected: $-1p$, $-1n$, $-d$, $-\alpha$, $+1n$, $+1p$, $+d$. Running the CCFUSB for each of the channels separately, only three of them came out as responsible for a reasonable enhancement of the sub-barrier fusion cross section: $-1p$, $-d$, $+d$. Actually, when these three channels are coupled to the fusion, the results are essentially the same as when one introduces the seven channels.

The $-1n$ channel, measured experimentally does not play an important role on fusion at sub-barrier energies. It has a large average transfer distance, of the order of $d_a = 1.72$ fm, a small slope parameter, $\langle \alpha \rangle = 0.50/\text{fm}$, and a negative Q_{eff} -value, -3.0 MeV.

The single channel responsible for the largest contribution to the fusion enhancement is the d ($\Delta D_t = 4.33$ MeV for $f = 2$), which has the largest Q_{eff} -value ($+7.9$ MeV), a relatively short average transfer distance ($\langle d_t \rangle = 1.65$ fm) and a steep

form factor ($\langle\alpha\rangle = 1.24/\text{fm}$). At the barrier its form factor is $F(r_b) = 0.426 \text{ MeV}$. Secondly comes the $+d$ channel, with the same transfer distance, $Q_{eff} = +2.9 \text{ MeV}$, $\langle\alpha\rangle = 1.13/\text{fm}$, $F(r_b) = 0.333 \text{ MeV}$ and $\Delta D_t = 2.16 \text{ MeV}$ for $f = 2$. The $-p$ channel has a large Q_{eff} -value ($+5.0 \text{ MeV}$), but as it takes place at larger distances ($\langle d_t \rangle = 1.69 \text{ fm}$) and it has a small form factor slope ($\langle\alpha\rangle = 0.56/\text{fm}$), the form factor at the barrier and the asymptotic shift are small compared with the $\pm d$ channels ($F(r_b) = 0.15 \text{ MeV}$ and $\Delta D_t = 1.0 \text{ MeV}$, for $f = 2$). Figure 4 also shows the results of the coupling of the inelastic channels and the $-d$, $+d$, $-1p$ transfer channels, for the values of $f = 1.0$ and 2.0 , on the fusion cross section. As there are no experimental data at low energies, only the predictions of the C.C. calculations can be used for a qualitative understanding of the process. The transfer of one deuteron, leading to intermediate projectiles 3α and 4α are predicted to be important doorways to fusion, and, as for the ^{16}O projectile, the stripping of one proton also plays some role on the fusion.

5. Summary and Conclusions

Fusion excitation functions were measured for the ^{14}N , $^{16}\text{O}+^{59}\text{Co}$ systems, at near barrier energies, and for the latter also at sub-barrier energies. Simultaneously, transfer cross sections to excited states of the $-1p$ and $-1n$ channels were measured for the ^{14}N induced reactions, and other transfer channels had the upper limits of their cross sections estimated. Elastic scattering for the $^{16}\text{O}+^{59}\text{Co}$ system was also measured. The following discussion will be focused on the $^{16}\text{O}+^{59}\text{Co}$ system. The first important fact to mention is that the sub-barrier fusion cross section enhancement for this light system was found to be as important as for heavy ones, as evidenced by the large value of η (the relative lowering of the Coulomb barrier needed to fit the experimental data).

The predicted enhancement of the fusion cross section for a spherical projectile and a target with small collectivity when one takes into account the dynamical defor-

mation of the nuclei (Wong model) or the alternative approach of coupling of inelastic channels are similar and very small. Nevertheless, a large fusion enhancement may arise from the neck formation process, or, from a microscopic view, the coupling of transfer channels.

In order to understand the role played by transfer channels on the fusion, several parameters must be considered, as the effective Q -value of the reaction, the average distance at which the transfers occur and the strength and slope of the form factors. For both systems studied in this work, the transfer of charged particles acting as doorways to fusion seems to be the main process responsible for the fusion enhancement, especially the stripping of multi-nucleons in which the form factors rise steeply at small distances and the effective Coulomb barrier is considerably lowered.

It is interesting to try to understand the whole reaction process in terms of distance parameters: for this system the Coulomb barrier is at $r_b = 1.48 \text{ fm}$; absorption starts to occur at $d_a = 1.74 \text{ fm}$; the average transfer distance for the $-\alpha$ channel is $\langle d_t \rangle = 1.59 \text{ fm}$; fusion starts to occur at r_f as far as 1.52 fm (from reference 9). The stripping of one alpha particle from the 4α projectile, at relatively short distances is, therefore, an important doorway to fusion.

The liquid drop approach to the neck formation and the coupling of transfer channels are shown to be equivalent, as well as the Wong model and the coupling of inelastic channels.

The conclusions obtained by the present analysis are in agreement with the ones obtained by the alternative formalism of direct reactions developed by Udagawa and collaborators¹⁰ where it was found⁹ that, for the $^{16}\text{O}+^{59}\text{Co}$ system, the part of the imaginary potential which accounts for the fusion is of long range, of the order of the Coulomb barrier. The additional attraction in the incident channel, giving rise to the sub-barrier fusion cross section enhancement can be understood as a consequence of strong absorption leading to fusion under or even outside the Coulomb barrier. During the multi-step fusion process a neck is formed.

We would like to thank Prof. S. Skorka for the SBTRANS and CCFUSB codes and the very useful suggestions and discussions about the coupled channel analysis and derivation of the form factors.

This work was partially financed by FINEP and CNPq.

References

- 1) Proceedings of the Symposium "Fusion Reaction Below the Coulomb Barrier", Cambridge, MA, 1984, in Lecture Notes in Physics, ed. S. Steadman, vol. 219 (Springer-Verlag, Berlin, 1985)
- 2) M. Beckerman, Phys. Rep. **129** (1985) 145
- 3) M. Beckerman, Rep. Prog. Phys. **51** (1988) 1047
- 4) Proceedings of the Symposium "Heavy Ion Interactions Around the Coulomb Barrier", Legnaro, 1988, in Lecture Notes in Physics, eds. C. Signorini, S. Skorka, P. Spolaore and A. Vitturi, vol. 317 (Springer-Verlag, Berlin, Heidelberg, New York, 1988)
- 5) C.H. Dasso and S. Landowne, Phys. Lett. **B183** (1987) 141
- 6) M. Beckerman, M. Saloma, A. Sperduto, J.D. Molitoris and A. Di Renzo, Phys. Rev. **C25** (1982) 837
- 7) K.E. Rehm, F.L.H. Wolfs, A.M. Van den Berg and W. Henning, Phys. Rev. Lett. **55** (1985) 280
- 8) C.H. Dasso, S. Landowne and A. Winther, Nucl. Phys. **A405** (1983) 381; R.A. Broglia, C.H. Dasso, S. Landowne and G. Pollarolo, Phys. Lett. **B133** (1983) 34
- 9) C. Tenreiro, P.R.S. Gomes, T.J.P. Penna, R. Liguori Neto, J.C. Acquadro, P.A.B. Freitas and E. Crema, Proceedings of the Workshop on Heavy Ion Collisions at Energies Near the Coulomb Barrier, Daresbury, 1990, in Inst. Phys. Conf. Ser. n. 110
- 10) T. Udagawa, T. Kim and T. Tamura, Phys. Rev. **C32** (1985) 124; T. Kim, T. Udagawa and T. Tamura, Phys. Rev. **C33** (1986) 370

- 11) P.R.S. Gomes, T.J.P. Penna, R. Liguori Neto, J.C. Acquadro, C. Tenreiro, P.A.B. Freitas, E. Crema, N. Carlin Filho and M.M. Coimbra, Nucl. Inst. Meth. Phys. Res. **280** (1989) 395
- 12) A. Gravon, Phys. Rev. **C21** (1980) 230
- 13) N.B.J. Tannous, J.F. Mateja, D.C. Wilson, L.S. Modsker and R.H. Davis, Phys. Rev. **C18** (1978) 2190
- 14) H.J. Krappe, J.R. Nix and A.J. Sierk, Phys. Rev. **C20** (1979) 992
- 15) J. Blocki, J. Randrup, W.J. Swiatecki and C.F. Tisang, Ann. Phys. **105** (1977) 427
- 16) L.C. Vaz, J.M. Alexander and G.R. Satchler, Phys. Rep. **69** (1981) 373
- 17) W. Reisdorf, F.P. Hessberger, K.D. Hildenbrand, S. Hoffman, G. Münzemberg, K.H. Schmidt, W.F.W. Schneider, K. Sümmerer, G. Wirth, J.V. Kratz, K. Schlitt and C.C. Sahn, Nucl. Phys. **A444** (1985) 154
- 18) C.E. Aguiar, V.C. Barbosa, L.F. Canto and R. Donangelo, Phys. Lett. **B201** (1988) 22; Nucl. Phys. **A472** (1987) 571
- 19) C.E. Aguiar, A.N. Aleixo, V.C. Barbosa, L.F. Canto and R. Donangelo, Nucl. Phys. **A500** (1989) 195
- 20) C.Y. Wong, Phys. Rev. Lett. **31** (1973) 766
- 21) P. Ring and P. Schuck, The Nuclear Many Body Problem, T.M.P. (Springer-Verlag, New York, Heidelberg, Berlin 1980)
- 22) E. Segre, Nuclei and Particles (Benjamin, New York, 1964)
- 23) S.J. Skorka, private communication
- 24) L. Corradi, S.J. Skorka, K.E.G. Löbner, P.R. Pascholati, U. Quade, K. Rudolph, W. Shomburg, M. Steinmayer, H.-G. Thies, G. Montagnoli, D.R. Napoli, A.M. Stefanini, A. Tivelli, S. Beghini, F. Scarlassara, C. Signorini and F. Soramel, Z. Physik **A344** (1990) 55
- 25) T. Winkelman, K. Balog, P. Jänker, H. Leitz, U. Lenz, K.E.G. Löbner, S.J. Skorka, M. Steinmayer, H.-G. Thies, L. Corradi, D.R. Napoli, A.M. Stefanini, S. Beghini, G. Montagnoli, F. Scarlassara, C. Signorini and F. Soramel, same Proceedings as in ref. 9
- 26) L.K. Peker, Nuclear Data Sheets **42** (1984) 457; P. Andersson, L.P. Ekström and J. Lyttkens, Nuclear Data Sheets **48** (1986) 251
- 27) S.J. Skorka, private communication
- 28) C.Y. Wu, X.T. Liu, W.J. Kernan, D. Cline, T. Czosnyka, M.W. Guidry, A.E. Kavka, R.W. Kincaid, B. Kotlinski, S.P. Sorensen and E. Vogt, Phys. Rev. **C39** (1989) 298
- 29) J. Wiggins, R. Brooks, M. Beckerman, S.B. Gazes, L. Grodzins, A.P. Smith, S.G. Steadman, Y. Xiao and F. Videbaek, Phys. Rev. **C31** (1985) 1315

Figure Captions

Figure 1 - Reduced fusion excitation functions for the $^{14}\text{N}+^{59}\text{Co}$ system, taken as reference, and for the $^{16}\text{O}+^{59}\text{Co}$. The solid line shows the prediction of the KNS model.

Figure 2 - Predictions from the uncoupled calculations (solid lines), inelastic channels coupling calculations (small dashed lines) and the Wong model (large dashed lines), for the $^{16}\text{O}+^{59}\text{Co}$ and $^{14}\text{N}+^{59}\text{Co}$ systems.

Figure 3 - Elastic over Rutherford differential cross sections as a function of the reduced distance of closest approach, for the $^{16}\text{O}+^{59}\text{Co}$ system, at $E_{\text{lab}} = 40$ MeV. The open square data are taken from reference 13.

Figure 4 - Coupled channel calculations for the ^{16}O and $^{14}\text{N}+^{59}\text{Co}$ systems. The full curves are the results without coupling. The dashed curves are the results of the coupling of inelastic and transfer channels, as described in the text.

Table Captions

Table 1 - Ground state transfer Q -values (Q_{gs}) and effective transfer Q -values ($Q_{eff} = Q_{gs} + \Delta E_c$) for transfer channels of one and two nucleons and one alpha particle for the ^{14}N , $^{16}\text{O}+^{59}\text{Co}$ systems. Stripping reactions are indicated by (-) and pick up reactions by (+).

Table 2 - Fusion and transfer cross sections measured for the ^{14}N , $^{16}\text{O}+^{59}\text{Co}$ systems.

Table 3 - Barrier parameters obtained from the fusion data above the Coulomb barrier by different unidimensional barrier penetration models, and values obtained from the systematics.

Table 1

	$^{14}\text{N} + ^{59}\text{Co}$		$^{16}\text{O} + ^{59}\text{Co}$	
	Q_{gs}	Q_{eff}	Q_{gs}	Q_{eff}
	MeV	MeV	MeV	MeV
-1n	- 3.06	- 2.90	- 8.17	- 8.32
-1p	+ 1.98	+ 5.02	- 2.59	- 0.28
-1 α	- 5.83	+ 0.25	- 1.38	+ 4.86
-2n	-13.80	-13.45	-12.07	-12.39
-2p	-10.85	- 4.40	- 8.01	- 1.95
-pn	+ 4.86	+ 7.75	- 5.61	- 2.89
+1n	+ 0.38	+ 0.27	- 6.31	- 6.17
+1p	- 0.07	- 2.81	- 6.73	- 8.10
+1 α	- 2.53	- 7.47	- 2.21	- 6.83
+2n	- 5.70	- 5.95	- 6.84	- 6.58
+2p	-12.55	-17.76	-14.79	-19.67
+pn	+ 5.55	+ 2.95	- 7.66	- 9.07

Table 2

E_{lab} *	E_{CM}	$\sigma_f(^{16}\text{O})$	$\sigma_f(^{14}\text{N})$	$\sigma_{tr}(-^{14}\text{N})$	$\sigma_{tr}(-^{14}\text{N})$
MeV	MeV	mb	mb	mb	mb
32	25.39		27.5 \pm 4.5	5.1 \pm 1.1	1.2 \pm 0.4
34	26.30	0.5 \pm 0.1			
	27.02		103 \pm 12	7.0 \pm 1.4	4.1 \pm 1.0
35	27.10	3.8 \pm 0.6			
36.5	29.06		299 \pm 40	10 \pm 2	7.0 \pm 1.5
40	31.00	88 \pm 14			
	31.90		558 \pm 68	14 \pm 2	6.5 \pm 1.8
45	35.96		730 \pm 75	20 \pm 3	10.0 \pm 2.5
48	38.40		901 \pm 80	21 \pm 4	11.0 \pm 2.5
50	39.00	527 \pm 63			
51	40.85		961 \pm 80	25 \pm 4	21 \pm 4
56	44.90		1113 \pm 113	23 \pm 4	20 \pm 4

*Not corrected by the energy loss in the target.

Table 3

System	Potential	V_B MeV	R_B fm	Δr fm	$\hbar\omega$ MeV
$^{16}\text{O} + ^{59}\text{Co}$	KNS	30.54	9.33	0	3.41
	Proximity	30.56	9.36	0.15	3.63
	Systematics	30.39	9.25		3.33
$^{14}\text{N} + ^{59}\text{Co}$	KNS	26.09	9.59	0.04	3.32
	Proximity	26.13	9.60	0.26	3.50
	Systematics	26.57	9.38		3.29

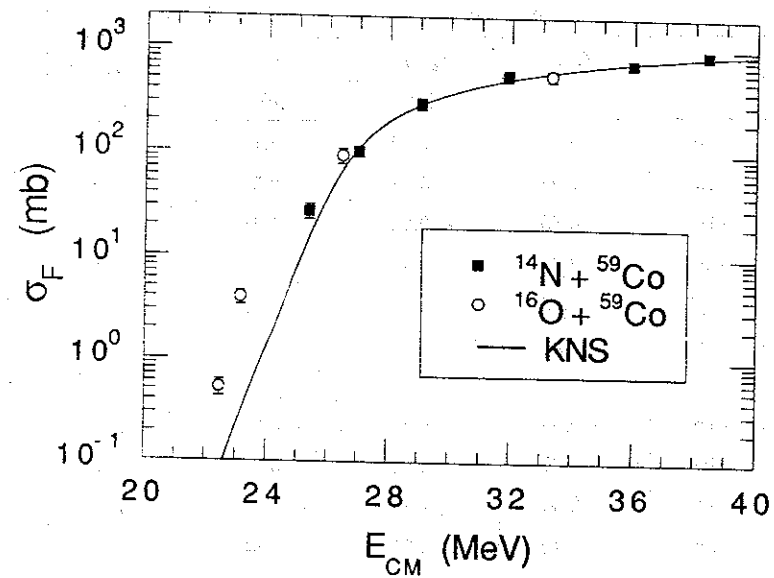


FIGURE 1

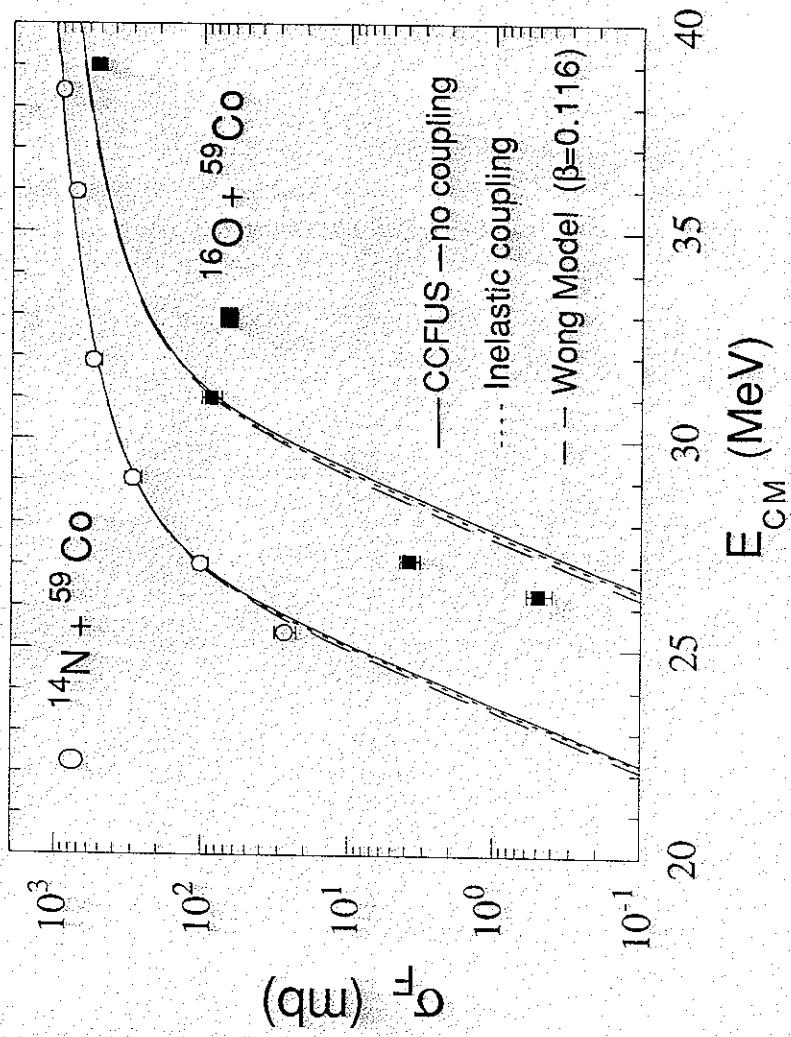


FIGURE 2

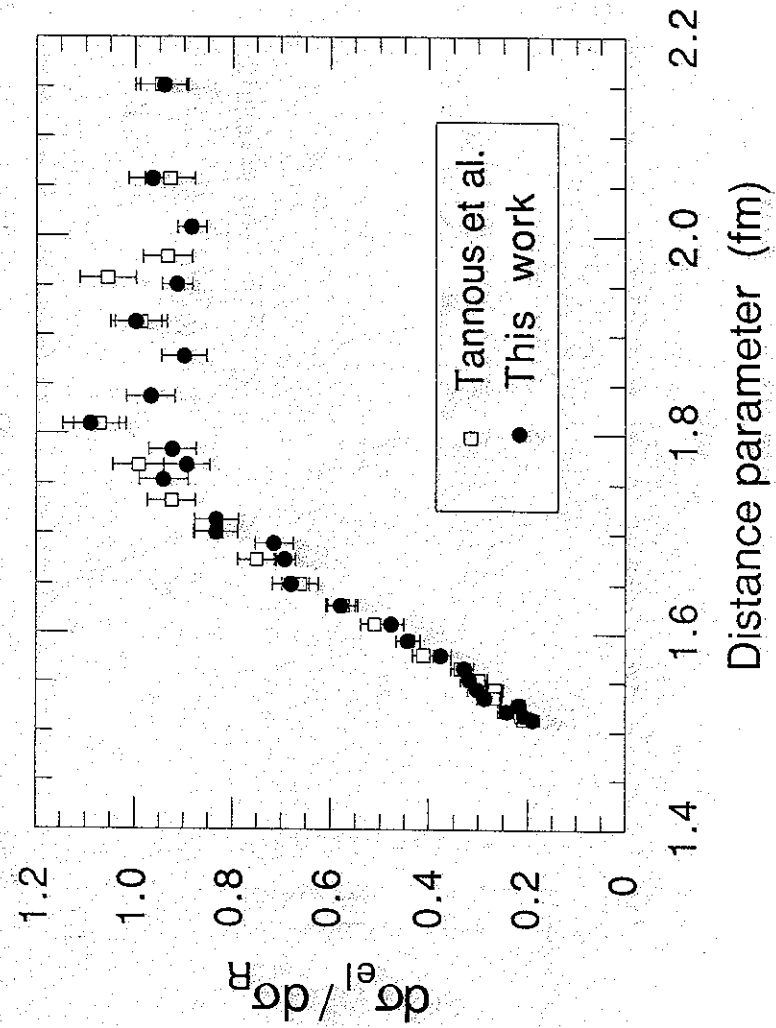


FIGURE 3

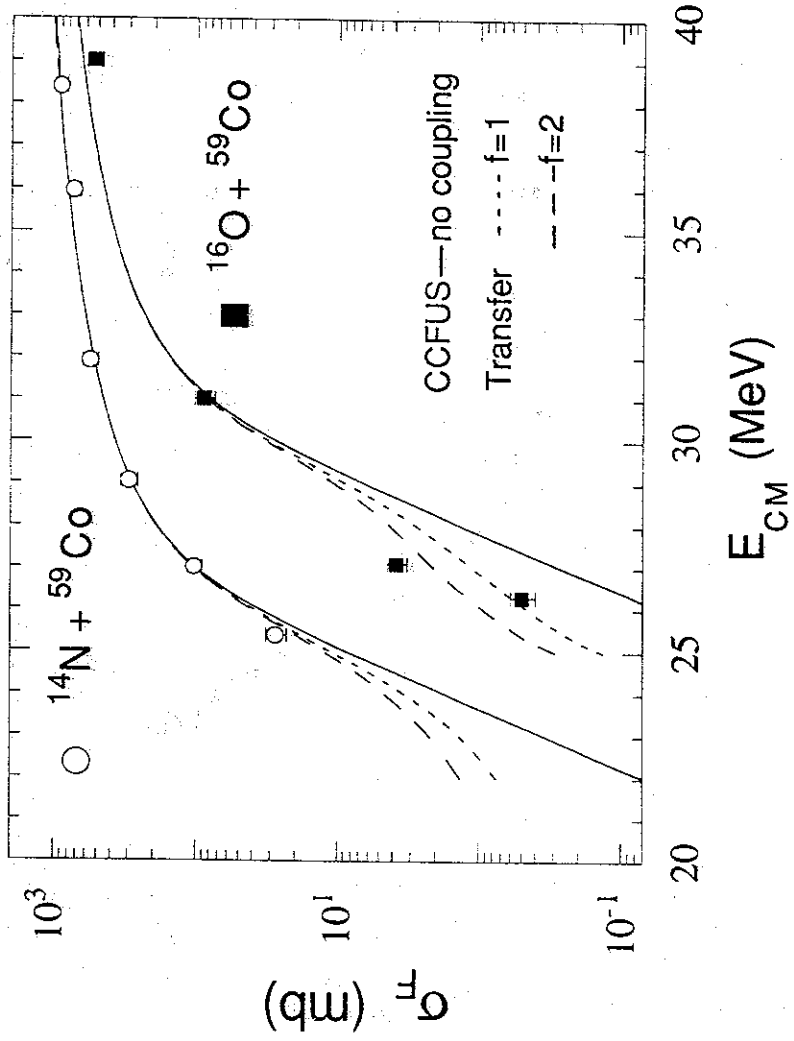


FIGURE 4

The figure shows the differential cross-section σ_F (mb) versus the center-of-mass energy E_{CM} (MeV) for the reactions $^{14}\text{N} + ^{59}\text{Co}$ and $^{16}\text{O} + ^{59}\text{Co}$. The y-axis is logarithmic, ranging from 10^{-1} to 10^3 mb. The x-axis is linear, ranging from 20 to 40 MeV. The data points are compared with theoretical curves for CCFUS (no coupling) and Transfer (with $f=1$ and $f=2$). The CCFUS curves are solid lines, and the Transfer curves are dashed lines. The $f=1$ curves are dashed with a longer dash, and the $f=2$ curves are dashed with a shorter dash. The $^{14}\text{N} + ^{59}\text{Co}$ data points are open circles, and the $^{16}\text{O} + ^{59}\text{Co}$ data points are filled squares. The data points generally follow the CCFUS curves, with some deviations at lower energies.